Available online at www.sciencedirect.com

ScienceDirect

Procedia CIRP 49 (2016) 113 – 120

www.elsevier.com/locate/procedia

The Second CIRP Conference on Biomanufacturing

Biomanufacturing of a chitosan/collagen scaffold to drive adhesion and alignment of human cardiomyocyte derived from stem cells

Patrizia Benzoni [a*], Paola Ginestra [b], Lina Altomare [c], Antonio Fiorentino [b], Luigi De Nardo [c], Elisabetta Ceretti [b], Patrizia Dell'Era [a]

1. a Dept. of Molecular and Translational Medicine University of Brescia - Health & Wealth, viale Europa 11, Brescia 25123, Italy
2. b Dept. of Mechanical and Industrial Engineering University of Brescia - Health & Wealth, via Branze 38, Brescia 25123, Italy
3. c Politecnico di Milano, Dept. of Chemistry, Materials, and Chemical Engineering "Giulio Natta", Via Mancinelli 7, Milano 20131, Italy

* Corresponding author. Tel.: 39 030 3717314; fax: +39 030 3717539. *E-mail address:* p.benzoni@unibs.it

Abstract

The in vitro generation of a three-dimensional (3D) myocardial tissue employing cells, biomaterials, and biomolecules is a promising strategy in cardiac tissue regeneration. Despite significant progresses in this field, cellular models are not yet able to provide a source of myocardial cells that will efficiently integrate and substitute damaged myocardial tissue. Stem cell-derived human cardiomyocytes (CMs) represent the most promising source for cardiac cell therapy. In order to sustain attachment, spreading, and orientation of human CMs on a scaffold we exploited an innovative negative replica patterning based on electrophoretic deposition to realize multi-scale micro-structured chitosan-collagen (C/C) scaffolds. Specific patterns were micro-structured on the cathode titanium disks using a laser machine. Cubic and hexagonal patterns were deeply characterized, and reproduced on the surface of the C/C scaffold. We initially challenged different blend with spontaneous contracting neonatal rat CMs to identificate the best substratum, finding that C/C 5:1 proportion can better sustain this type of culture. Finally, human CMs derived from induced pluripotent stem cells were seeded on these patterned scaffolds and colonization of the substrate was observed, thus confirming the validity of the chosen biomaterial. Moreover, preliminary experiments demonstrate the effectiveness of the pattern in controlling the orientation of human CMs.

In conclusion, we designed and fabricated a scaffold that allows the attachment, spreading, and orientation of human CMs due to a correct C/C blend composition, to an innovative manufacturing process, and to an effective 3D architecture of the patterns. These data will surely help in solving the quest for a cardiac clinical patch.

Peer-review under responsibility of the scientific committee of The Second CIRP Conference on Biomanufacturing

Keywords: Cardiomyocytes; Laser micro-machining; Electrophoretic deposition; Biomaterial

1. Introduction

During embryonic development, cardiac cells undergo a complex series of structural changes that ultimately lead to their adult phenotype. This process is regulated in vivo by different factors, including environmental cues such as extracellular matrix, soluble factors, mechanical signals and electrical fields that may determine the emergence of spatial patterns that will lead to tissue morphogenesis.

The comprehension of early growth and maturation processes of cardiac tissue in humans is difficult, due in part to limitations in obtaining a sufficient number of cells. Indeed, cardiomyocytes in the postnatal human heart are essentially post-mitotic, precluding their cultivation and expansion in vitro and, on the other hand, fetal human heart tissue is difficult to obtain. The capability to reprogram patient-derived somatic cells to induced pluripotent stem cells (iPSC) and direct their differentiation toward cardiomyocytes (iPSC-CMs) has provided large-scale cultures of human cardiomyocytes to generate powerful platform for regenerative medicine, development, tissue engineering, disease modeling, and drug toxicity testing [1].

IPSC-CMs beat spontaneously, express cardiac sarcomeric proteins and ion channels, exhibit

Peer-review under responsibility of the scientific committee of The Second CIRP Conference on Biomanufacturing
doi:10.1016/j.procir.2015.09.004

cardiac-type action potentials and calcium transients. Despite these promising results, many lines of evidence indicate that in the currently used conditions, iPSC-CMs do not exhibit the morphological and functional characteristics of adult CMs. Thus, to maximize the hypothetical therapeutic benefits of using these cells for regenerative medicine purposes, a critical challenge is to enhance their maturation status mimicking nature's work. On this basis, the present research started to explore the possibility to provide a three-dimensional environment that improves cellular organization and crosstalk using tissue-engineering techniques [2].

The selection of biomaterial/scaffold with topographical features is a crucial step to achieve a favorable environment for cell growth and tissue development. The material utilized in building such cellular support must be biocompatible with cell attachment sites and an interconnected porous structure that allows nutrients and waste cellular products exchanges [3]. Moreover, in order to support cardiac cell contraction, peculiar mechanical strength, stiffness and elasticity are required [4]. In this study, we designed and tested a chitosan/collagen (C/C) blend matrix with large interconnected pores, that has already been shown to possess the required mechanical, structural, and compositional features to be used in different advanced tissue regeneration applications [5; 6]. Chitosan has a cationic nature allowing electrostatic interactions with anionic glycosaminoglycans (GAG) and proteoglycans of the extracellular matrix. Furthermore, in blend with collagen type I, can be resolved in different structures and micro-patterned to modulate adhesion and maturation of cells [7]. To enhance the alignment of cells, the C/C scaffold was design to incorporate an array of ridges and grooves. It has already been demonstrated that two-dimensional micro-pattern shape may play a role in controlling sarcomere morphology of human cardiomyocytes derived from embryonic stem cells. In particular it was determined that a range between 30 μm and 80 μm is the ideal ridge width to promote alignment of immature human embryonic stem cell-derived CMs thus resulting in improved sarcomere formation [8]. Similar features were investigated also in three-dimensional scaffolds. Kolowe et al. [9] proposed a rectangular pore pattern (125 μm × 250 μm inner pore dimensions with 50μm structure width and 70 μm thick) deposed on a flat surface, demonstrating multiscale alignment of C2C12 myoblasts [9]. The use of rectangular pores in the scaffold design was motivated by their bi-dimensional mechanical anisotropy, similar in structure to native adult rat ventricular myocardium [10; 11]. On these bases, a regular patterned C/C matrix was designed, manufactured by electrophoretic deposition of the blend on titanium disk, previously patterned using laser micro-ablation and finally tested.

2. Production and characterization of C/C scaffold

2.1 Electrophoretic deposition: scaffold fabrication

Chitosan-collagen scaffolds were produced by electrophoretic deposition as elsewhere described [12]. A flat titanium foil was used as cathode to obtain porous scaffold, while titanium laser-machined foils described below were used to obtain micro-patterned scaffolds. A solution of medium molecular weight chitosan isolated from shrimp shell (Sigma-Aldrich 417963, 75-85% de-acetylated) 0.1% (w/v) in acetic acid (ACS reagent, ≥99.7%, Sigma-Aldrich 320099) at two different pHs (3 and 3.5) was obtained; two different amount of collagen from rat-tail were dissolved in chitosan solution to obtain a chitosan/collagen ratio of 5:1 and 3:1.

The electrophoretic deposition (EPD) was performed by using a power supply (100 W Source Meter, Keithley 2425) in the following optimized conditions: porous scaffolds were deposited in galvanostatic conditions at 10 mA/cm^2 for 20 minutes at pH 3.5, while patterned scaffolds were deposited in potentiostatic conditions by applying a square waveform of 90 V for 25 seconds and 100 V for 5 seconds at pH 3 for 20 minutes. This latter condition has been optimized in order to control the deposition inside the grooves of the pattern at the beginning of EPD avoiding in this phase the evolution of big hydrogen bubbles due to the reduction process at the cathode.

After the deposition, the scaffolds were gently washed in distilled water and left overnight in NaOH 1M to allow an easily peeling off the cathode. The morphology of the porous scaffolds was evaluated by scanning electron microscope (SEM) StereoScan® 360 at 10 kV and their mechanical properties were evaluates as elsewhere reported [12]. Before cells seeding, the scaffolds were sterilized with 70% ethanol and UV light for 20 minutes, washed with phosphate buffered saline (PBS) (Invitrogen, Carlsbad, CA, USA). In order to improve the adhesion of CMs, scaffold were coated with fibronectin (10 μg/ml) by a 40 minutes dip at room temperature.

2.2 Pattern definition and generation

The two pattern configurations are constituted by an intersection of grooves: cubic rectangular (CR) and hexagonal rectangular (HR), indicating

four and six first-neighbor pores respectively that are formed by the grooves, as shown in Fig. 1.

The groove dimensions are: 50 µm width (w), 100 µm deep, while each rectangular pore formed by the grooves is 125 µm x 250µm (l x L). The whole pattern has a 5x5 mm^2 area.

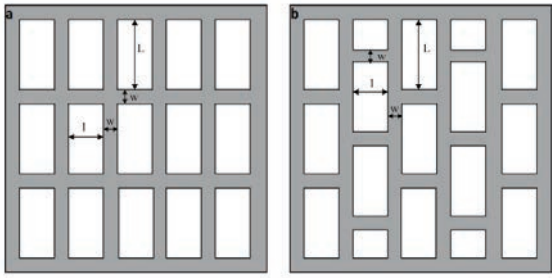

	l (µm)	L (µm)	w (µm)	depth (µm)
CR pattern	125	250	50	100
HR pattern	125	250	50	100

Fig. 1: Imposed pattern configurations: cubic (a) and hexagonal (b) and their geometrical parameters respectively

A LEP Lee Laser (Nd:YVO4, 8 W q-switched, λ= 532 nm) was used during the experimental campaign for ablating these specific patterns on titanium disks (commercially pure grade II, clean in acetic acid), round shaped (Ø=10 mm), 0.5 mm thick. The high quality beam (M^2=1) can work at pulse frequency of 200 kHz and pulse minimum duration of 12 ns.

The laser machine is controlled by a software where it is possible to set the scan speed, the q-switch frequency, the duty cycle, the laser path strategy, the beam diameter, the loop number of cycles of ablation and the laser power expressed as the percentage of the applied current to the pump system (diode lasers). Since the laser is controlled in current, preliminary calibration tests were conducted to optimize micro machining process [13].

In particular, a cycle of ablation on 25 mm^2 area was used and a power meter (Gentec-EO UP19-W) was executed to convert the percentage Ampere in average power. Table 1 reports the parameters and equations needed to test if the power density is able to ablate the titanium or not through the fluence per pulse [14; 15].

Table 1. Direct and indirect laser parameters.

Parameter	Description	Value or Equation
f [kHz]	q-switch frequency	30,100
Pavg [W]	average power	2.64, 1.45, 0.35
v_s [mm/s]	scan speed	381, 304.8, 228.6
d [mm]	spot diameter	0.6
Abs [%]	absorption coefficient	
dt [ns]	pulse width	$t = \frac{dc}{f}$
dc [%]	duty cycle	
Ppeak [W]	peak power	$P_{peak} = \frac{P_{avg}10^{-6}}{f \cdot dt}$
tloop [s]	time per loop	$t_{loop} = \frac{Area}{d} \cdot \frac{1}{v_s}$
Epulse [J]	energy per pulse	$E_{pulse} = P_{avg} \cdot dt$
F pulse [J/cm^2]	fluence per pulse	$F_{pp} = abs \cdot \frac{4}{\pi d^2} \cdot E_{pulse}$

The outgoing laser beam is collimated in a galvo system to impose a remote control. Each titanium disk was fixed on a frame at a distance equal to the focal distance (160 mm) from the galvo head. The experiments set designed to obtain the two selected configurations were conducted as reported in Table 2.

Table 2. Designed laser-machining cycle.

Process parameter	Set value
f [kHz]	30
dt [ns]	104
v_s[mm/s]	2.64
dc [%]	30
Ppeak [W]	8.80
Fpulse [J/cm^2]	0.56
# loop	30

Each ablation cycle was repeated for several times to reach the desired configuration depth. As it can be observed, each cycle reaches a value of fluence per pulse value that is higher than ablation threshold for titanium alloy equal to 0.109 J/cm^2 [16]. Moreover, five test repetitions with the same parameters were carried out to study the laser cycle effects on channels configuration homogeneity in terms of width and depth distributions.

2.3 Pattern characterization

The titanium samples surface was observed using Zeiss LEO EVO 40 scanning electron microscope (SEM) to analyze the laser modification performed on an area of 25 mm^2. To reveal the cross-sections, Mitutoyo Quick Scope QS-200z optical microscope system equipped with a 7X objective was used. The observed samples demonstrated a surface morphology depending on the configuration imposed as shown in Fig. 2.

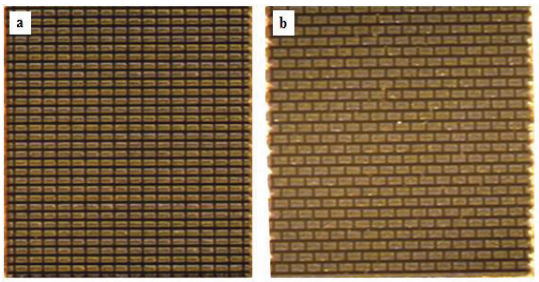

Fig. 2. Optical microscope images 2x of configuration CR(a) and HR (b) (25 mm^2 Area).

Moreover, the images from SEM at high magnification were analyzed with AxioVs40 V 4.8.2.0 software to obtain data on the imposed configuration dimensions and channel homogeneity (Fig. 3). Measurements were taken considering the refund material that reconstitutes the channel cross-section, as it possible to detect in the crop detail (Fig. 3c). The channel wall exhibits a conical cross-section from the bottom (black) to the top (light grey) due to Gaussian distribution of the laser spot that leads to a great amount of refund material piled on the side of the marking line after each loop. Reaching a total depth of 100 µm causes plasma emission: a certain quantity of vaporized material remains within the channel due to the high shape ratio chosen between line width (50 µm) and desired depth (100 µm). For this reason the cross-section periodic morphology was analyzed in five tests resulted in high standard deviation (Fig. 3d).

These results suggest that surfaces are characterized by different shapes of furrows that will be analyzed properly in future tests. Pure Argon will be chosen as assist gas to reduce piled material through an homogeneous flux oriented at 45° with respect to the specimen.

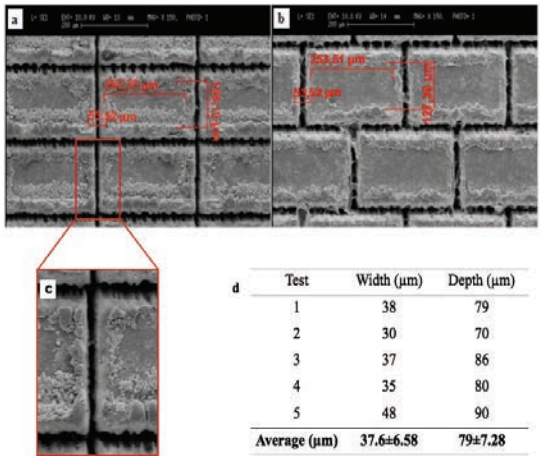

Test	Width (µm)	Depth (µm)
1	38	79
2	30	70
3	37	86
4	35	80
5	48	90
Average (µm)	37.6±6.58	79±7.28

Fig.3. (a,b) SEM images 150X of CR and HR configurations with the relative real measurements (µm) referred to l, L and w values reported in Fig.3. (c) Crop detail of configuration CR showing channel cross-section detail. (d) Laser machining quality results.

2.4 Scaffold Characterization

In Fig. 4, patterned vs. porous EPD scaffolds are shown. The random porosity due to hydrogen formation during EPD is homogeneously and uniformly distributed between the two blends (5:1 and 3:1). Analyzing the SEM images of porous scaffolds deposited on flat titanium with AxioVs40 V 4.8.2.0 software, a slightly pores size reduction has been noticed related to increasing collagen amount (mean size of 68,8 ± 34,65 µm and 31,64 ± 19,01 µm for 5:1 C/C and 3:1 C/C scaffolds respectively). Nevertheless, this difference doesn't change the mechanical property in terms of elastic modulus between the two scaffolds (E=1,56 ±0,29 MPa and 1,42 ±0,62 MPa, respectively).

For patterned scaffold only the C/C concentration 5:1 was used for two different patterns, as previously described. Both patterns were well replicated and it is still visible the presence of pores due to hydrogen production, even though the application of the square wave allows a faster release of bubbles from the surface of titanium thus controlling the micro porosity of the growing ridges at the beginning of the EPD.

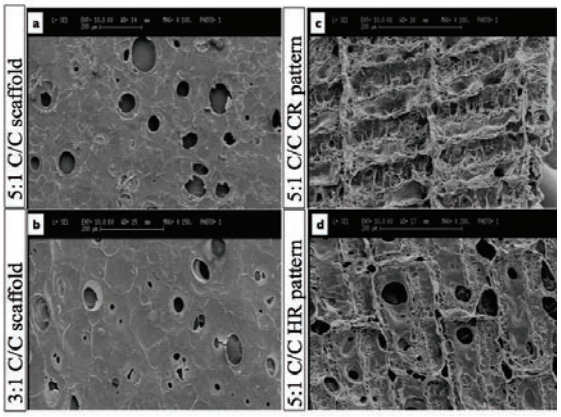

Fig. 4. Different kind of scaffolds obtained by EPD analyzed by SEM. (a, b) Random porous scaffolds with different collagen amount. (c, d) Patterned scaffolds in which the CR (c) and HR (d) configuration are replicated.

The thickness of the obtained scaffolds allows an easy handling of the final structure (205 ± 30 µm and 180 ± 29 µm for 5:1 C/C and 3:1 C/C scaffolds respectively) in the following cell seeding, resulting in the suitable microstructural features for the exchange of cellular nutrients and wastes [17].

3. Cells and C/C scaffold interaction

In order to analyze the biocompatibility of the C/C material, two different cell lines was tested. To determine the influence of the scaffold on cell viability, we use a cell line of human foreskin fibroblasts (HFF) with a high duplication rate. Then, we moved to mouse myoblasts C2C12, again an easy-handling cell line closer to our CM model, to test the adhesive capacity.

Cultures were trypsinized and resuspended as single cells at high cellular density (1000 cells/µl). A small drop of cell suspension (50 µl) was deposited on top of the rehydrated scaffold inserted in a 35 mm Petri dish and incubated for 2 hours before filling the plate with a proper volume of culture medium. In our experience this process strongly enhances cell attachment. After 3 days the C/C scaffolds were fixed in 4% paraformaldehyde (PFA) for 5 minutes and stained with DAPI that marks the nuclei and DiI (Life Technologies) that marks the lipid membrane. Indeed, as shown by fluorescence microscopy images (Fig. 5) high cellular seed density using either HFF or C2C12 was obtained. In particular, as shown by DiI staining of cellular membranes, both cell lines are spread inside the scaffold, which implies active cellular interaction with the matrices, thus strengthening the evidence of C/C biocompatibility.

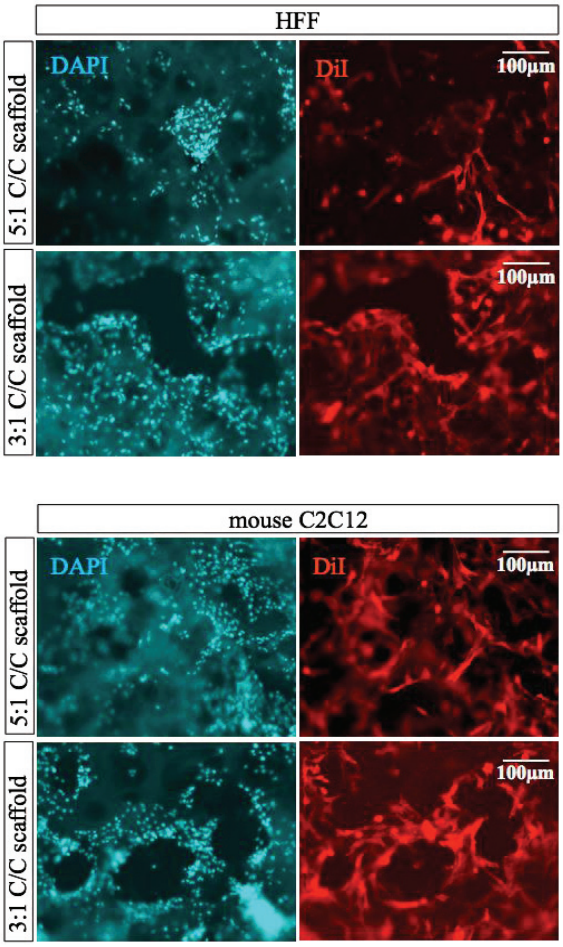

Fig. 5. Fluorescent microscopy of HFF and mouse myoblasts C2C12 seeded on C/C scaffold 5:1 and 3:1, nuclei staining with DAPI (blue) and cell membrane staining with DiI (red). 5X magnification.

Further investigations were conducted on the cell-scaffold interaction using a primary culture of rat neonatal cardiomyocytes (rCM), which is closer to human iPSC-derived CMs that we intend to use to build the engineered tissues, showing a spontaneous contractility.
Cardiomyocytes were isolated from 2-day-old neonatal rats as previously reported [18] Briefly, rat ventricles were quartered, washed, and incubated in Hank's balanced salt solution (HBSS) with 3mM $CaCl_2$ and subjected to a series of digestions (10 minutes, 37 °C in a warm bath) in HBSS using 100 U/ml collagenase type IV and 0,4 mg/ml pancreatin. Cell suspensions from the first 4–5 digestions were collected in cold FBS and centrifuged at 300 rpm for 10 minutes. The supernatant was removed; cells were resuspended in culture medium and subjected to a pre-plating step for 1 h to get rid of quickly adherent cardiac fibroblasts.

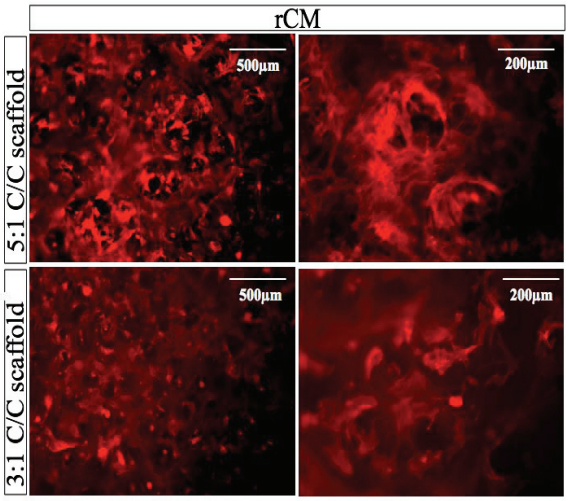

Fig. 6. Fluorescent microscopy of neonatal rat cardiomyocytes seeded on C/C scaffold 5:1 and 3:1, stained with Phalloidin-543 that marks the cytoskeletal actin filaments.

Isolated CMs were seeded in air-dried fibronectin-coated scaffolds as previously described. Actin filament staining of the samples (Fig. 6) shows that also rCM are able to attach and spread on C/C scaffolds. Nevertheless, the scaffold with larger pores (5:1 blend) seems to better sustain the survival of rCM. Indeed, a synchronous spontaneous contraction of rCM was obtained that confirms the wide spreading and connection of the rCM in this condition. This result qualify the 5:1 scaffold as the best option for cardiac cell culture, probably due to its porosity, allowing valuable cell inter-connection, and sufficient nutrient and oxygen diffusion. Therefore, for the following experiments using human cardiomyocytes only this latter C/C

scaffold was investigated and patterned as reported previously.

Human iPSC lines already produced in our laboratory are used to generate the large numbers of human cardiomyocytes required for cardiac tissue patch fabrication and testing. Specifically, iPSC were cultured in 12 well plates as pluripotent colony until they reach 60-70% of confluence, then induced to differentiate using the commercially available PSC Cardiomyocyte Differentiation Kit (Life Technologies). Spontaneously contracting syncytium of iPSC-CMs can appear as early as 10 days later. Isolated iPSC-CMs after two weeks of culture exhibited a cross-striated phenotype known to support the contraction and expression of cardiac functional genes. 14-day old iPSC-CMs were trypsinized in small cluster and seeded in air-dried fibronectin-coated scaffolds with and without CR pattern.

Even if the distribution of cells is not homogeneous, as with rCM, adequate colonized scaffolds showing spontaneous beating in different areas were obtained. In particular, the presence of CR pattern orientates iPSC-CMs in areas with higher cellular density. This data was confirmed by analyzing the orientation of sarcomeric protein Troponin T (Fig. 7a,b). The measurement of cell orientation was analyzed in order to evaluate the effect of the pattern.

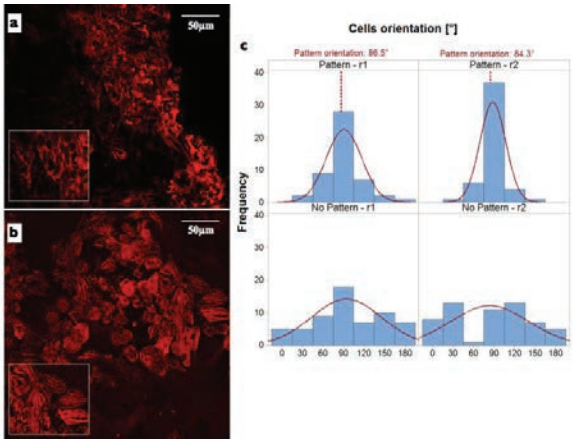

Fig. 7. (a,b) Fluorescent microscopy of human cardiomyocytes stained for cardiac troponin T in red seeded onto the C/C scaffold with and without CR pattern respectively. (c) Histograms showing orientations of patterns (red dots line, measured along the long side of pattern) and orientations of cardiac troponin in different cells

The results reported in Fig.7c show that without a guided groove cells tend to spread in all directions while when the pattern is adopted, iPSC-CMs regulate the cytoskeletal orientation according to the design (red dots line). Since the fitted Gaussian distribution (continuous red line) do not show a reliable data approximation, distribution identification tests were performed in order to identify which types of statistical distributions characterized the cell orientations. These tests transform the data in a Normal distribution N(0;σ=1) under the assumption that they follow a specific distribution and evaluate the goodness of fit (p-value) of the transformed data.

The results (Table 3) confirms that the data are not Gaussian (low p-values for the normal transformation), while Johnson Transformation is the best for all the cases. In particular, different transformation functions were identified (Fig. 8): *arcsinh* function, in case of the results with the pattern and *ln* function in the ones without and it is very effective on pattern data.

From the comparison of the results, it is possible to observe that:

- *No pattern*. Cell orientations (Fig. 7c) do not show significant symmetry or trend. Moreover, no good results were obtained in the identification of their statistical distribution (Table 3 and Fig. 8). Finally, the *logarithmic* transformation, which has the effect of concentrating the data on their average value, show that they are more uniformly spread with respect to the Gaussian distribution. These aspects suggest that cells naturally tend to spread along any direction with the same probability.
  Since further equal probability tests did not confirm this conclusion, it is possible that inhomogeneities in the scaffolds (bubbles, roughness) locally influence the cell orientations thus modifying their distribution.

Table 3. Goodness of Fit Test

	p-values			
	Pattern		*No Pattern*	
Transformation	*r1*	*r2*	*r1*	*r2*
Normal	0.042	<0.05	0.129	<0.05
Box-Cox Transform.	0.054	<0.05	0.129	<0.05
Lognormal	0.008	<0.05	<0.05	<0.05
Exponential	<0.03	<0.03	<0.03	<0.03
2-Parameter Exponent.	<0.10	<0.10	<0.10	<0.10
Weibull	<0.10	<0.10	<0.10	<0.10
3-Parameter Weibull	0.019	<0.05	0.074	<0.05
Smallest Extreme Value	<0.10	<0.10	0.012	<0.10
Largest Extreme Value	<0.10	<0.10	<0.10	<0.10
Gamma	0.04	<0.0	<0.0	<0.0

	3	05	05	05
Logistic	>0.2 50	0.01 9	0.07 2	<0.0 05
Log logistic	0.10 4	<0.0 05	<0.0 05	<0.0 05
Johnson Transformation	0.93 6	0.84 1	0.20 1	0.10 3

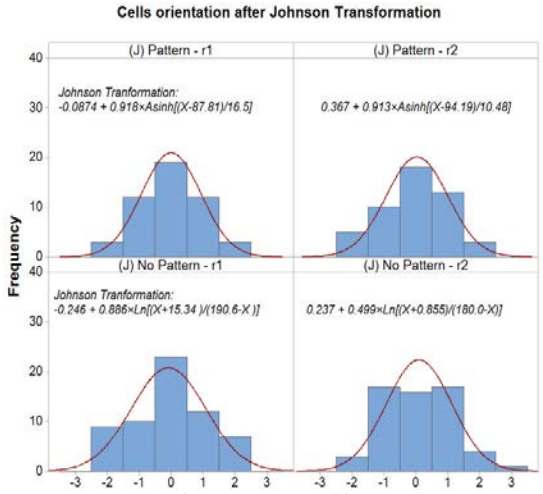

Fig. 8. Functions used for the Johnson transformation and distribution of the transformed data on cell orientations.

- *With pattern*. Cell orientations (Fig. 7c) follow the pattern direction. Moreover, the *arcsinh* transformation spreads the data from their average to the tails of the distribution (Fig. 8), which means that they are more concentrated along the pattern direction with respect to a Gaussian. In particular, this confirms the strong influence of the pattern on cell orientations.

4. Conclusion

Here we proposed a technological process where different expertise are put together to solve the clinical need for cardiac patches, designed to embed therapeutic cells in suitable matrices that support cell adhesion and survival. The main cell types constituting human heart comprise fibroblasts, endothelial cells, and mainly cardiomyocytes (CMs), post-mitotic cells with poor culture plasticity. Indeed, while it's relatively easy to separate and cultivate the first two cell types, isolated human adult CMs do not survive as much in culture. Thus, we setup a protocol that allows CM differentiation from induced pluripotent stem cells and use these precious cells to verify a series of parameters already determined with fibroblasts, myoblasts, and primary neonatal rat CMs.

The designed scaffold is based on a blend of chitosan and collagen that offers a variety of unexplored opportunities for supporting cardiac tissues: new processing technologies such as electrophoretic deposition, and the possibility to realize in situ hierarchical structures with tunable patterning and porosities. The scaffold supports fibroblasts as well as myoblasts adhesion and proliferation, thus being highly biocompatible. The following seeding of rat CMs, only after fibronectin coating, showed a favored spreading, survival, and intra-cellular connection of this type of cells on the 5:1 C/C combination, thus showing a preference for the substrate with larger porosity. Since the myocardium is composed by oriented fibers, it was tested whether 3D architectural cues could be used to align stem cell-derived human CMs.

A preliminary application of a LEP Lee Laser for manufacturing periodic micro-topography with variable geometrical parameters on titanium disks that allowed us to obtain a scaffold mold, with precise and repeatable patterns was reported too. The micro-fabricated master, representing the cathode with a negative pattern replicated by the deposition process, can be used for several cycles thus making this process timesaving. Future studies on surfaces with controlled architecture will be considered for precise description of the relation between imposed laser configuration parameters on the final surface structure. Moreover, optimization campaigns will be carried out in order to evaluate the shape parameters of the grooves obtained on titanium samples.

Although preliminary data are shown, in this study we demonstrate attachment, spreading, and orientation of human CMs due to a correct C/C blend composition, to an innovative manufacturing process that implies electrodeposition of the material in a mold, and to an effective 3D architecture. Moreover, data on cell orientations show the effectiveness of the pattern in controlling cell adhesion. These data will surely help in solving the quest for a cardiac clinical patch.

References

[1] Novakovic GV, Eschenhagen T and Mummery C. Myocardial Tissue engineering: in vitro models. Cold Spring Harb Perspect Med 2014; 4:a04076.

[2] Yang X, Pabon L, Murry CE. Engineering adolescence: maturation of human pluripotent stem cell-derived cardiomyocytes. Circ Res. 2014; 114(3):511-23.

[3] Chien KR, Domian IJ, Parker KK. Cardiogenesis and the complex biology of regenerative cardiovascular medicine. Science 2008; 322(5907):1494-7.

[4] Bouten CV, Dankers PY, Driessen-Mol A, Pedron S, Brizard AM, Baaijens FP. Substrates for cardiovascular tissue engineering. Adv Drug Deliv Rev. 2011;63(4-5):221-41.

[5] Kim IY, Seo SJ, Moon HS, Yoo MK, Park IY, Kim BC, Cho CS. Chitosan and its derivatives for tissue engineering applications. Biotechnol Adv 2008; 26:1-21.

[6] Zhang T, Wan LQ, Xiong Z, Marsano A, Maidhof R, Park M, Yan Y, Vunjak-Novakovic G. Channelled scaffolds for engineering

myocardium with mechanical stimulation. J Tissue Eng Regen Med. 2012;6(9):748-56.
[7] Wang H, Shi J, Wang Y, Yin Y, Wang L, Liu J, Liu Z, Duan C, Zhu P, Wang C. Promotion of cardiac differentiation of brown adipose derived stem cells by chitosan hydrogel for repair after myocardial infarction. Biomaterials. 2014; 35(13):3986-98.
[8] Salick MR, Napiwocki BN, Sha J, Knight GT, Chindhy SA, Kamp TJ, Ashton RS, Crone WC. Micropattern width dependent sarcomere development in human ESC-derived cardiomyocytes. Biomaterials. 2014 May; 35(15):4454-64.
[9] Kolewe ME, Park H, Gray C, Ye X, Langer R, Freed LE. 3D structural patterns in scalable, elastomeric scaffolds guide engineered tissue architecture. Adv Mater. 2013; 25(32):4459-65.
[10] Engelmayr GC Jr, Cheng M, Bettinger CJ, Borenstein JT, Langer R, Freed LE. Accordion-like honeycombs for tissue engineering of cardiac anisotropy. Nat Mater. 2008; 7(12):1003-10.
[11] Park H, Larson BL, Guillemette MD, Jain SR, Hua C, Engelmayr GC Jr, Freed LE. The significance of pore microarchitecture in a multi-layered elastomeric scaffold for contractile cardiac muscle constructs. Biomaterials. 2011; 32(7):1856-64.
[12] Altomare L, Guglielmo E, Varoni EM, Bertoldi S, Cochis A, Rimondini L & De Nardo L. Design of 2D chitosan scaffolds via electrochemical structuring. Biomatter. 2014; 4:1, e29506.
[13] Giorleo L., Ceretti E., Giardini C. Ti surface laser polishing: effect of laser path and assist gas. 9th CIRP Conference on Intelligent Computation in Manufacturing Engineering - CIRP ICME '14, Capri, Italy, 23-25 July 2014.
[14] Tang G, Abdolvand A. Structuring of titanium using a nanosecond-pulsed Nd:YVO4 laser at 1064 nm. Inter J of Adv Man Tech. 2013; 66:1769–1775.
[15] The Essential Physics of Medical Imaging , Jerrold T. Bushber; 1994.
[16] Zheng B, JiangG, WangW, Wang K, Mei X. Ablation experiment and threshold calculation of titanium alloy irradiated by ultra-fast pulse laser. Micromachines 2015, 6(1):19-3.
[17] Radisic M, Park H, Chen F Salazar-Lazaro JE, Wang Y, Dennis R, Langer R, Freed LE, Vunjak-Novakovic G. Biomimetic Approach to Cardiac Tissue Engineering: Oxygen Carriers and Channeled Scaffolds. Tissue engineering, August 2006, 12(8): 2077-2091.
[18] Radisic M, Park H, Martens TP, Salazar-Lazaro JE, Geng W, Wang Y, Langer R, Freed LE, Vunjak-Novakovic G. Pre-treatment of synthetic elastomeric scaffolds by cardiac fibroblasts improves engineered heart tissue. J Biomed Mater Res A. 2008 ; 86(3):713-24.